Resource Allocation for Wireless Communication Networks with RF Energy Harvesting

Elena Boshkovska

Friedrich-Alexander-University Erlangen-Nürnberg (FAU), Germany

Derrick Wing Kwan Ng

The University of New South Wales, Australia

Robert Schober

Friedrich-Alexander-University Erlangen-Nürnberg (FAU), Germany

CONTENTS

1.1 INTRODUCTION

The successful development of wireless communication networks and technologies has triggered an exponential growth in the number of wireless communication devices worldwide. In the near future, devices embedded with multifunctional sensors and communication chip sets will be able to collect and exchange information via the Internet. Specifically, these smart devices will be connected to computationally powerful central computing systems to provide

intelligent services for the daily life such as environmental monitoring, e-health, automated control, energy management, logistic, and safety management. This new concept of interconnecting a massive number of communication and sensing devices is known as the Internet of Things (IoT) [1].

It is predicted that in 2020, the number of devices interconnected via the Internet on the planet may reach up to 50 billion. Besides, the density of such networks will be around 1 million devices per km^2. Therefore, the wireless communication infrastructure is a key enabler of IoT. In fact, IoT requires energy-efficient and cost effective wireless communications. Similar to conventional communication networks, the lifetime of IoT networks depends on the available energy at the transceivers. However, smart devices in IoT networks are ubiquitous with various levels of mobility. In other words, connecting these devices to fixed power grids to replenish their energy may not be a viable option. Therefore, most of the transceivers in IoT networks will be powered by batteries with limited energy storage which will reduce the lifetime of the networks significantly. Although the energy shortage can be alleviated by temporary battery replacements, such an intermediate solution may require frequent replacement of batteries which can be costly, time consuming, and cause interruption of service. This creates a serious performance bottleneck for providing stable communication, especially for delay sensitive services. On the other hand, a viable solution to extend the lifetime of wireless communication networks is to integrate wireless communication devices with energy harvesting (EH) technology to scavenge energy from the environment. In practice, wind, solar, and geothermal are the major renewable energy sources for generating electricity [2, 3, 4], thereby reducing substantially the reliance on the energy supply from the power grid. Yet, these conventional natural energy sources are usually climate and location dependent which restricts the mobility of smart devices. Besides, most of these energy sources are not available in indoor environments. More importantly, the uncontrollable and intermittent nature of these natural energy sources makes their use in IoT communication networks challenging.

Recently, wireless energy transfer (WET) has emerged as one of the technologies driving IoT networks and has attracted much attention from both academia and industry [5]–[27]. The existing WET technologies can be categorized into three classes: inductive coupling, magnetic resonant coupling, and radio frequency (RF)-based WET. The first two technologies rely on near-field electromagnetic (EM) waves. In particular, these two technologies can provide wireless charging over short distances only due to the required alignment of the magnetic field with the EH circuit. Therefore, in general, near-field techniques do not support the mobility of EH devices. In contrast, RF-based WET [5]–[24] exploits the far-field properties of EM waves facilitating long distance wireless charging. More importantly, EM waves not only serve as a vehicle for carrying energy, but also for carrying information which enables the possibility of simultaneous wireless information and power transfer (SWIPT) and wireless powered communication (WPC). Specifically, in SWIPT networks, a transmitter broadcasts both information and energy signals to provide information and energy delivery service simultaneously. In wireless powered communication networks (WPCNs), wireless communication devices first harvest energy, either from a dedicated power station or from ambient RF signals, and then use the harvested energy to transmit information signals. Compared to conventional EH, RF-based EH technology provides an on-demand energy replenishment which is suitable for smart wireless communication devices having strict quality of service (QoS) and energy requirements. On the other hand, various "last meter" wireless communication systems, such as Wi-Fi and small cell systems, can be potentially exploited for energy replenishment of battery constrained wireless devices. Nowadays, simple EH circuits are able to harvest microwatts to milliwatts of power over the range of several meters for a transmit power of 1 Watt and a carrier frequency of less than 1 GHz [28]. Although the development of WET technology is still in its infancy, there are already some preliminary practical applications of

WET such as passive radio-frequency identification (RFID) systems. It is expected that the introduction of RF-based EH to smart communication devices will revolutionize the system architecture and resource allocation algorithm design.

Conventional wireless communication systems are required to provide different types of QoS requirements such as throughput, reliability, energy efficiency, fairness, and timeliness [29]–[32]. On top of this, efficient WET is expected to play an important role as an emerging QoS requirement for RF-based wireless EH communication networks. In practice, for a carrier frequency of 915 MHz, the signal attenuation is 50 dB for every 10-meter of free space propagation. Hence, the efficiency of WET will be unsatisfactory for long distance transmission unless advanced resource allocation and antenna technology are combined. As a result, various resource allocation algorithms exploiting multiple-antenna technology have been proposed [17]–[24]. Specifically, by utilizing the extra degrees of freedom offered by multiple transmit antennas, a narrow signal beam can be created and can be more accurately steered towards the desired receivers to improve the efficiency of WET. In this chapter, we study the resource allocation algorithm design for two specific RF-based multiple antenna EH communication networks.

The remainder of this chapter is organized as follows. In Section 1.2, we introduce various types of receiver structures for RF-based EH wireless communications. Sections 1.3 and 1.4 study the resource allocation algorithm design for SWIPT systems and WPCNs , respectively. In Section 1.5, we conclude with a brief summary of this chapter.

Notation

In this chapter, we adopt the following notations. $\mathbf{A}^H$, $\mathrm{Tr}(\mathbf{A})$, and $\mathrm{Rank}(\mathbf{A})$ represent the Hermitian transpose, trace, and rank of matrix $\mathbf{A}$; $\mathbf{A} \succeq \mathbf{0}$ indicates that $\mathbf{A}$ is a positive semidefinite matrix; matrix $\mathbf{I}_N$ denotes an $N \times N$ identity matrix. $\mathrm{vec}(\mathbf{A})$ denotes the vectorization of matrix $\mathbf{A}$. $\mathbf{A} \otimes \mathbf{B}$ denotes the Kronecker product of matrices $\mathbf{A}$ and $\mathbf{B}$. $[\mathbf{B}]_{a:b,c:d}$ returns a submatrix of $\mathbf{B}$ including the a-th to the b-th rows and the c-th to the d-th columns of $\mathbf{B}$. $[\mathbf{q}]_{m:n}$ returns a vector with the m-th to the n-th elements of vector $\mathbf{q}$. A complex Gaussian random vector with mean vector $\boldsymbol{\mu}$ and covariance matrix $\boldsymbol{\Sigma}$ is denoted by $\mathcal{CN}(\boldsymbol{\mu}, \boldsymbol{\Sigma})$, and $\sim$ means "distributed as". $\mathbb{C}^{N \times M}$ denotes the space of all $N \times M$ matrices with complex entries. $\mathbb{H}^N$ represents the set of all N-by-N complex Hermitian matrices. $\mathcal{E}\{\cdot\}$ denotes statistical expectation. $|\cdot|$, $\|\cdot\|$, and $\|\cdot\|_{\mathrm{F}}$ denote the absolute value of a complex scalar, the Euclidean norm, and the Frobenius norm of a vector/matrix, respectively; $\mathrm{Re}\{\cdot\}$ denotes the real part of an input complex number.

1.2 RECEIVER STRUCTURE

Wireless communications via propagating EM waves in RF enables the possibility of SWIPT and WPC which is foreseen to be a key technology for facilitating the development of IoT communication networks with energy-limited wireless transceivers. Yet, the utilization of EM waves as a carrier for SWIPT and WPC poses many new research challenges for receiver design. Early studies on SWIPT and WPCNs were based on a pure information theoretical approach [5, 33]. In particular, it was assumed in these works that information decoding and EH can be performed based on the same received signal and an ideal receiver. However, this is not possible in practice, yet. Specifically, existing EH circuits extract the energy of the received signal in the RF domain. The EH process destroys the information content embedded in the signal. Besides, conventional information decoding is performed in the digital baseband and frequency down converted signals cannot be used for EH. As a result, various types of practical EH receivers have been proposed to enable SWIPT. In particular, for SWIPT, the
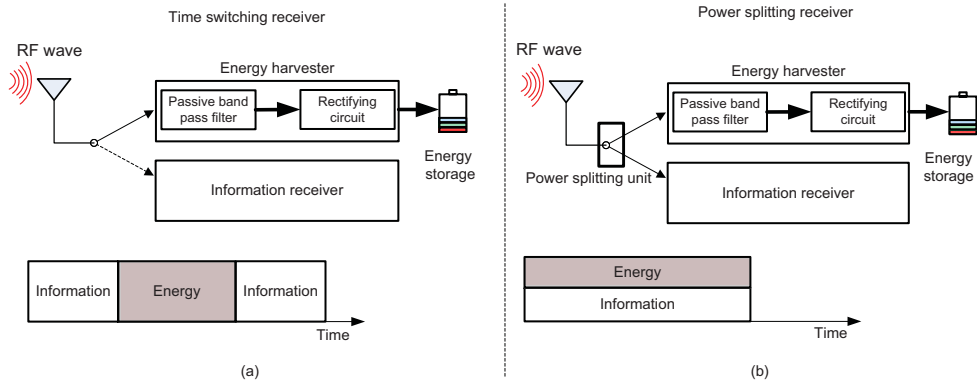
Figure 1.1 Simple receiver structures for wireless information and power transfer; (a) Time switching receiver; (b) Power splitting receiver.

information decoding process and EH process have to be separated. A viable solution is to split the received RF power into two distinct parts, one for EH and one for information decoding. In the following, we discuss two commonly adopted techniques to achieve this signal splitting.

Time Switching (TS) Receiver:

With TS receivers, each transmission block is divided into two orthogonal time slots, one for transferring wireless power and the other one for transmitting information, cf. Figure 1.1a. The co-located energy harvester and information receiver switch between harvesting energy and decoding in two time slots [17]. In practice, by taking into account the channel statistics and QoSs for power transfer, the time durations for wireless information transfer and energy transfer can be optimized to achieve different system design objectives. Although the TS receiver structure allows for a simple hardware implementation, it requires accurate time synchronization and information/energy scheduling, especially in multi-user systems.

Power Splitting (PS) Receiver:

A power splitting (PS) receiver splits the signal received at the antenna into two streams at different power levels using a PS unit, cf. Figure 1.1b. In particular, one stream is sent to the RF energy harvester for EH, and the other one is converted to baseband for information decoding [17, 19]. The PS process incurs a higher receiver complexity compared to the TS process. Besides, optimization of the ratio of the two power streams is needed in order to achieve a balance between the performances of information decoding and EH. Furthermore, additional noise may be introduced due to the adopted PS process [14]. Nevertheless, this receiver structure achieves SWIPT, as the signal received in one time slot is exploited for both information decoding and power transfer. Therefore, it is more suitable than the TS receiver for applications with critical information/energy or delay constraints [6].

In the sequel, we study the resource allocation algorithm design for two practical wireless information and power transfer networks based on the TS receiver structure, due to its simpler hardware implementation. Since the unit of "Joule-per-second" is used for energy consumption in this chapter, the terms "power" and "energy" are interchangeable.

1.3 SWIPT COMMUNICATION NETWORKS

In this section, we outline the adopted system model for the considered SWIPT systems.
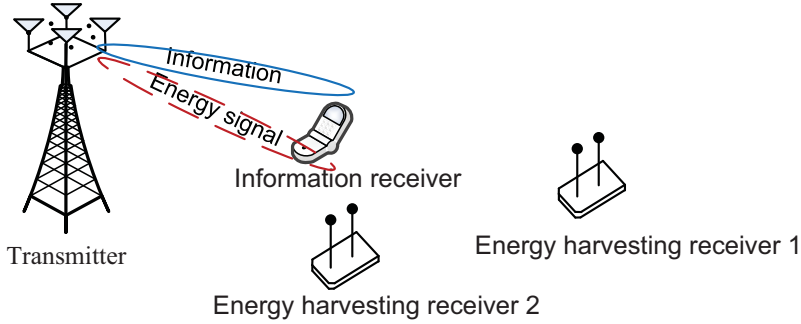
Figure 1.2 A simple SWIPT system model with one information receiver and $J = 2$ EH receivers (ERs), e.g. wireless sensors. The ERs harvest energy from the received RF signals to extend their lifetimes.

1.3.1 Channel Model

A frequency flat fading communication channel is considered. The SWIPT system comprises a transmitter, an information receiver (IR), and J EH receivers (ER)[1], cf. Figure 1.2. The transmitter is equipped with $N_T \geq 1$ antennas and serves both the IR and the ERs simultaneously in the same frequency band. We assume that the IR is a single-antenna device for assuring low hardware complexity. Each ER is equipped with $N_R \geq 1$ receive antennas to facilitate wireless EH. The received signals at the IR and ER $j \in \{1, \dots, J\}$ are given by

$$
\begin{aligned}
y &= \mathbf{h}^H \mathbf{w} s + \mathbf{w}_E + n, \text{ and} & (1.1)\\
\mathbf{y}_{ER_j} &= \mathbf{G}_j^H \mathbf{w} s + \mathbf{w}_E + \mathbf{n}_{ER_j}, \ \forall j \in \{1, \dots, J\}, & (1.2)
\end{aligned}
$$

respectively, where $s \in \mathbb{C}$ and $\mathbf{w} \in \mathbb{C}^{N_T \times 1}$ are the data symbol and the information beamforming vector, respectively. Without loss of generality, we assume that $\mathcal{E}\{|s|^2\} = 1$. The channel vector between the transmitter and the IR is denoted by $\mathbf{h} \in \mathbb{C}^{N_T \times 1}$ and the channel matrix between the transmitter and ER j is denoted by $\mathbf{G}_j \in \mathbb{C}^{N_T \times N_R}$. $n \sim \mathcal{CN}(0, \sigma_s^2)$ and $\mathbf{n}_{ER_j} \sim \mathcal{CN}(\mathbf{0}, \sigma_s^2 \mathbf{I}_{N_R})$ are the additive white Gaussian noises (AWGN) at the IR and ER j, respectively, where σ_s^2 denotes the noise power at the receiver. $\mathbf{w}_E \in \mathbb{C}^{N_T \times 1}$ is a Gaussian pseudo-random sequence generated by the transmitter to facilitate efficient wireless power transfer. In particular, $\mathbf{w}_E$ is modelled as a complex Gaussian random vector with

$$
\mathbf{w}_E \sim \mathcal{CN}(\mathbf{0}, \mathbf{W}_E), \tag{1.3}
$$

where $\mathbf{W}_E \in \mathbb{H}^{N_T}, \mathbf{W}_E \succeq \mathbf{0}$, denotes the covariance matrix of the pseudo-random energy signal.

1.3.2 Non-linear Energy Harvesting Model

In this section, we discuss two mathematical models used in the literature to capture the characteristic of practical RF EH circuits. To this end, we first study a basic approach for extracting electrical energy from the received RF signals. In practice, after the transmitted RF signal is received at the antenna(s) of an ER, a passive bandpass filter is employed before the received RF signal is passed on to a rectifying circuit, cf. Figure 1.1. In fact, the rectifying circuit is the core element of RF EH circuits. In particular, it is a passive electronic circuit

---

[1]The considered system can be treated as having $J + 1$ TS receivers where one of the receivers is in the IR mode and the remaining J receivers are in the ER mode.

comprising diodes, resistors, and capacitors that converts the incoming RF power to direct current (DC) power. Then, the converted power can be stored in the energy storage unit of the receiver.

The RF-to-DC energy conversion efficiency depends greatly on the characteristics of the rectifying circuit. In general, rectifiers can be implemented using different non-linear circuits, starting from the simplest half-wave rectifiers, cf. Figure 1.3, to complicated circuits that offer N-fold increase of the circuit output power so as to improve the efficiency of the circuit, cf. Figure 1.4. A half-wave rectifier, as depicted in Figure 1.3, passes either the positive or negative half of the alternating current (AC) wave, while the other half is blocked [34]. Although half-wave rectifiers result in a lower output voltage compared to other types of rectifiers, a half-wave rectifier requires only a single diode and is a very simple design. Thus, half-wave rectifiers are suitable for cheap and small mobile devices such as wireless sensors for IoT applications. On the other hand, Figure 1.4 depicts an array of voltage doubler circuits, where each part of the circuit consists of two diodes and other corresponding elements. Depending on the number of stages required for a particular rectifier, the circuit parts can be repeated until the N-th element is reached. This configuration offers an increase of the conversion efficiency of the circuit.

In general, one can derive mathematical equations to describe the input-output characteristic of an EH circuit based on its schematic, e.g. Figures 1.3 and 1.4. However, they usually lead to complicated expressions which are intractable for resource allocation algorithm design. More importantly, such an approach relies on specific implementation details of EH circuits and the corresponding mathematical expressions may differ significantly across different types of EH circuits. In the following, we discuss two general tractable models proposed in the literature for characterizing the aforementioned RF EH process. Mathematically, the total received RF power at ER j is given by

$$P_{\mathrm{ER}_j} = \mathrm{Tr}\left((\mathbf{w}\mathbf{w}^H + \mathbf{W}_{\mathrm{E}})\mathbf{G}_j\mathbf{G}_j^H\right). \tag{1.4}$$

In the SWIPT literature [36]–[44], the total harvested power at ER j, $\Phi_{\mathrm{ER}_j}^{\mathrm{Linear}}$, is typically modelled by the following linear equation:

$$\Phi_{\mathrm{ER}_j}^{\mathrm{Linear}} = \eta_j P_{\mathrm{ER}_j}, \tag{1.5}$$

where $0 \leq \eta_j \leq 1$ is the constant power conversion efficiency of ER j. In other words, the total harvested power at the ER is linearly and directly proportional to the received RF power. Besides, the total harvested power increases with the amount of received power without bound.

Yet, practical RF-based EH circuits introduce non-linearities into the end-to-end WET and the conventional linear model fails to capture this important characteristic, as shown by experimental results [35, 45, 46]. Recently, a parametric non-linear EH model was proposed in [24, 47] to facilitate the design of resource allocation algorithms for practical SWIPT systems. Here, the total harvested power at ER j, Φ_{ER_j}, is modelled as:

$$\Phi_{\mathrm{ER}_j} = \frac{[\Psi_{\mathrm{ER}_j} - M_j\Omega_j]}{1 - \Omega_j}, \ \Omega_j = \frac{1}{1 + \exp(a_j b_j)}, \tag{1.6}$$

$$\text{where } \Psi_{\mathrm{ER}_j} = \frac{M_j}{1 + \exp\left(-a_j(P_{\mathrm{ER}_j} - b_j)\right)} \tag{1.7}$$

is a logistic function which has the received RF power, P_{ER_j}, as the input. In particular, three parameters, i.e., M_j, a_j, and b_j, are introduced to describe the shape of the logistic
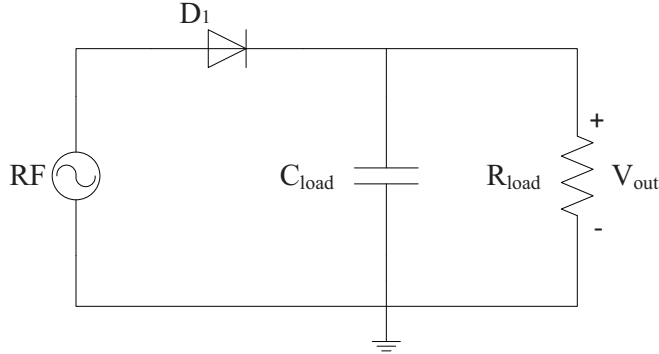
Figure 1.3 A schematic of a half-wave rectifier [35] where C_{load}, R_{load}, D_1, and V_{out} denote a load capacitance, load resistance, diode, and the output voltage, respectively.
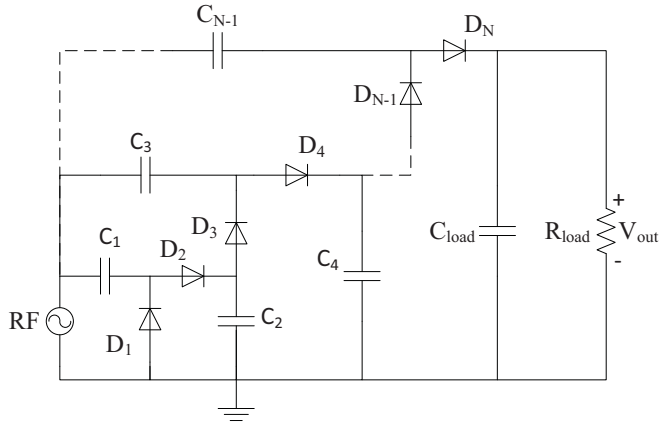

Figure 1.4 A schematic of a Dickson charge pump [35] with N stages, where D_i, and C_i, $i \in \{1, \dots, N\}$, denote the diode and the capacitor in the i-th stage.

function which depends on various physical properties of the RF EH circuit. Specifically, M_j is a positive constant denoting the maximum harvestable power at ER j, when the EH circuit is saturated due to an exceedingly large input power. Parameters a_j and b_j are constants which capture the joint effects of resistance, capacitance, and circuit sensitivity. Specifically, a_j denotes the non-linear charging rate with respect to the input power and b_j is related to the minimum turn-on voltage of the EH circuit.

In practice, for a given EH hardware circuit, the values of parameters a_j, b_j, and M_j of the proposed model in (1.6) can be estimated by using a standard curve fitting algorithm. In Figure 1.5, we show an example for the curve fitting for the non-linear EH model in (1.6) with parameters $M = 0.024$, $b = 0.014$, and $a = 150$. As can be observed, the parametric non-linear model matches the experimental result provided in [45] closely for the RF power harvested by a practical EH circuit. For comparison, Figure 1.5 also illustrates the total harvested power predicted by the linear model in (1.5). It can be seen that the conventional linear RF energy harvesting model fails to capture the non-linear characteristics of practical EH circuits, especially in high and low received RF power regimes.
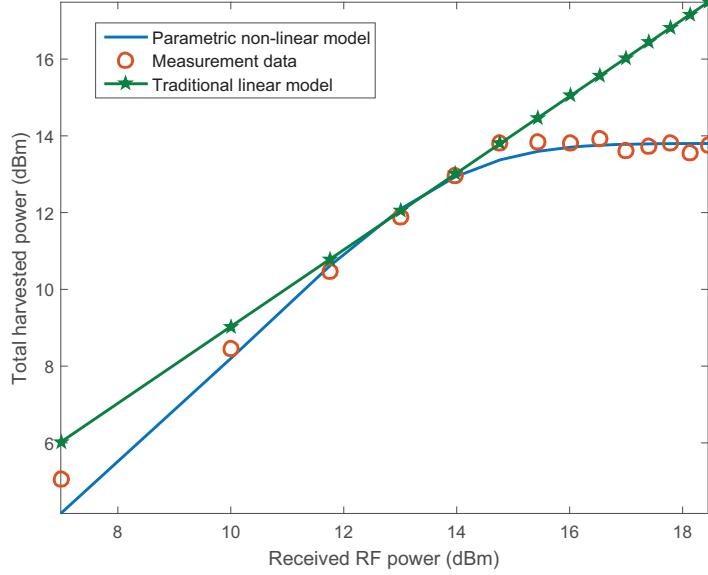
Figure 1.5 A comparison between experimental data from [45], the harvested power for the non-linear model in (1.6), and the linear EH model with $\eta_j = 0.8$ in (1.5).

1.3.3 Channel State Information

We assume that only imperfect channel state information (CSI) is available at the transmitter for resource allocation due to the slow time varying nature of the communication channels. To capture the impact of the CSI imperfection on resource allocation design, we adopt a commonly used deterministic model [19, 20]. In particular, the CSI of the links between the transmitter and the information receiver as well as EH receiver j can be modelled as:

$$\mathbf{h} = \widehat{\mathbf{h}} + \Delta\mathbf{h}, \tag{1.8}$$

$$\boldsymbol{\Upsilon} \triangleq \left\{ \Delta\mathbf{h} \in \mathbb{C}^{N_{\mathrm{T}}\times 1} : \|\Delta\mathbf{h}\|_2^2 \leq \rho^2 \right\}, \tag{1.9}$$

$$\mathbf{G}_j = \widehat{\mathbf{G}}_j + \Delta\mathbf{G}_j, \ \forall j \in \{1,\ldots,J\}, \ \text{and} \tag{1.10}$$

$$\boldsymbol{\Xi}_j \triangleq \left\{ \Delta\mathbf{G}_j \in \mathbb{C}^{N_{\mathrm{T}}\times N_{\mathrm{R}}} : \|\Delta\mathbf{G}_j\|_{\mathrm{F}}^2 \leq \upsilon_j^2 \right\}, \forall j, \tag{1.11}$$

respectively, where $\widehat{\mathbf{h}}$ and $\widehat{\mathbf{G}}_j$ are the estimates of channel vector $\mathbf{h}$ and channel matrix $\mathbf{G}_j$, respectively. $\Delta\mathbf{h}$ and $\Delta\mathbf{G}_j$ represent the channel uncertainty due to channel estimation errors. In (1.9) and (1.11), sets $\boldsymbol{\Upsilon}$ and $\boldsymbol{\Xi}_j$ define the continuous spaces spanned by all possible channel uncertainties, respectively. Constants ρ and υ_j denote the maximum value of the norm of the CSI estimation error vector $\Delta\mathbf{h}$ and the CSI estimation error matrix $\Delta\mathbf{G}_j$, respectively.

Remark 1 *In practical systems, the values of ρ^2 and υ_j^2 depend not only on the adopted channel estimation method, but also on the packet duration and the coherence time of the associated communication channel.*

1.3.4 Achievable System Data Rate

The energy signal $\mathbf{w}_{\mathrm{E}}$ is a Gaussian pseudo-random sequence which is known to all the transceivers. Hence, interference cancellation can be performed at the IR to facilitate information decoding. As a result, given perfect CSI at the receiver for coherent information decoding, the achievable rate (bit/s/Hz) between the transmitter and the IR is given by

$$R \;=\; \log_2\left(1 + \frac{|\mathbf{h}^H\mathbf{w}|^2}{\sigma_{\mathrm{s}}^2}\right), \tag{1.12}$$

where the interference caused by the energy signal, i.e., $\mathrm{Tr}(\mathbf{h}^H\mathbf{W}_{\mathrm{E}}\mathbf{h})$, has been removed.

1.3.5 Problem Formulation and Solution

In the considered SWIPT system, we aim to maximize the total achievable data rate of the system while guaranteeing a minimum total harvested power at multiple ERs. The resource allocation algorithm design is formulated as the following optimization problem:

Problem 1 Robust Resource Allocation for SWIPT:

$$\underset{\mathbf{w},\mathbf{W}_{\mathrm{E}}\in\mathbb{H}^{N_{\mathrm{T}}}}{\mathrm{maximize}} \;\; \underset{\Delta\mathbf{h}\in\boldsymbol{\Upsilon}}{\min} \quad \log_2\left(1 + \frac{|\mathbf{h}^H\mathbf{w}|^2}{\sigma_{\mathrm{s}}^2}\right) \tag{1.13}$$

$$\text{subject to} \quad \text{C1}: \; \|\mathbf{w}\|_2^2 + \mathrm{Tr}(\mathbf{W}_{\mathrm{E}}) \leq P_{\max},$$

$$\text{C2}: \; \underset{\Delta\mathbf{G}_j\in\boldsymbol{\Xi}_j}{\min} \Phi_{\mathrm{ER}_j} \geq P_{\mathrm{req}_j}, \forall j \in \{1,\dots,J\}.$$

The objective function in (1.13) takes into account the CSI uncertainty set $\boldsymbol{\Upsilon}$ to provide robustness against CSI imperfection. Constants $P_{\max}$ and P_{req_j} in constraints C1 and C2 are the maximum transmit power from the power station and the required minimum harvested power at ER j, respectively. It can be observed that there are infinitely many possibilities in both the objective function and constraint C2, due to the CSI uncertainties. In order to design a computationally efficient resource allocation algorithm, we first define $\mathbf{W} = \mathbf{w}\mathbf{w}^H$ and transform the considered problem into the following equivalent rank-constrained semi-definite program (SDP):

Problem 2 Rank-constrained Robust Resource Allocation for SWIPT:

$$\underset{\mathbf{W},\mathbf{W}_{\mathrm{E}}\in\mathbb{H}^{N_{\mathrm{T}}},\tau,\boldsymbol{\beta}}{\mathrm{maximize}} \quad \tau \tag{1.14}$$

$$\text{subject to} \quad \text{C1}: \; \mathrm{Tr}(\mathbf{W} + \mathbf{W}_{\mathrm{E}}) \leq P_{\max},$$

$$\text{C2}: \; M_j \geq \Theta_j\Big(1 + \exp\big(-a_j(\beta_j - b_j)\big)\Big), \forall j \in \{1,\dots,J\},$$

$$\text{C3}: \; \underset{\Delta\mathbf{h}\in\boldsymbol{\Upsilon}}{\min} \mathrm{Tr}(\mathbf{W}\mathbf{H}) \geq \tau,$$

$$\text{C4}: \; \underset{\Delta\mathbf{G}_j\in\boldsymbol{\Xi}_j}{\min} \mathrm{Tr}\big((\mathbf{W} + \mathbf{W}_{\mathrm{E}})\mathbf{G}_j\mathbf{G}_j^H\big) \geq \beta_j, \forall j \in \{1,\dots,J\},$$

$$\text{C5}: \; \mathrm{Rank}(\mathbf{W}) \leq 1,$$

$$\text{C6}: \; \mathbf{W} \succeq \mathbf{0},$$

$$\text{C7}: \; \mathbf{W}_{\mathrm{E}} \succeq \mathbf{0},$$

---

where

$$\Theta_j = P_{\text{req}_j}(1 - \Omega_j) + M_j\Omega_j \quad \text{and} \tag{1.15}$$

$$\mathbf{H} = \mathbf{h}\mathbf{h}^H. \tag{1.16}$$

$\boldsymbol{\beta} = \{\beta_1, \ldots, \beta_j, \ldots, \beta_J\}$ and τ are auxiliary optimization variables. We note that $\mathbf{W} \succeq \mathbf{0}$, $\mathbf{W} \in \mathbb{H}^{N_\text{T}}$, and $\text{Rank}(\mathbf{W}) = 1$ in (1.14) are imposed to guarantee that $\mathbf{W} = \mathbf{w}\mathbf{w}^H$ after optimization. Now, the transformed problem in (1.14) involves infinitely many constraints only in C3 and C4. Besides, the rank constraint in C5 is non-convex. To further facilitate the solution, we first transform constraints C3 and C4 into linear matrix inequalities (LMIs) using the following lemma:

Lemma 1 (S-Procedure [48]) *Let a function $f_m(\mathbf{x}), m \in \{1, 2\}, \mathbf{x} \in \mathbb{C}^{N \times 1}$, be defined as*

$$f_m(\mathbf{x}) = \mathbf{x}^H \mathbf{A}_m \mathbf{x} + 2\text{Re}\{\mathbf{b}_m^H \mathbf{x}\} + c_m, \tag{1.17}$$

where $\mathbf{A}_m \in \mathbb{H}^N$, $\mathbf{b}_m \in \mathbb{C}^{N \times 1}$, and $c_m \in \mathbb{R}$. Then, the implication $f_1(\mathbf{x}) \leq 0 \Rightarrow f_2(\mathbf{x}) \leq 0$ holds if and only if there exists a $\delta \geq 0$ such that

$$\delta \begin{bmatrix} \mathbf{A}_1 & \mathbf{b}_1 \\ \mathbf{b}_1^H & c_1 \end{bmatrix} - \begin{bmatrix} \mathbf{A}_2 & \mathbf{b}_2 \\ \mathbf{b}_2^H & c_2 \end{bmatrix} \succeq \mathbf{0}, \tag{1.18}$$

provided that there exists a point $\hat{\mathbf{x}}$ such that $f_m(\hat{\mathbf{x}}) < 0$.

Exploiting Lemma 1, the original constraint C3 holds if and only if there exists a $\delta \geq 0$, such that the following LMI constraint holds:

$$\text{C3: } \mathbf{S}_{\text{C}_3}\big(\mathbf{W}, \delta, \tau\big) = \begin{bmatrix} \delta \mathbf{I}_{N_\text{T}} & \mathbf{0} \\ \mathbf{0} & -\delta\rho^2 - \tau \end{bmatrix} + \mathbf{U}_{\hat{\mathbf{h}}}^H \mathbf{W} \mathbf{U}_{\hat{\mathbf{h}}} \succeq \mathbf{0}, \tag{1.19}$$

where $\mathbf{U}_{\hat{\mathbf{h}}} = \begin{bmatrix} \mathbf{I}_{N_\text{T}} & \hat{\mathbf{h}} \end{bmatrix}$. Similarly, constraint C4 can be equivalently written as

$$\text{C4: } \mathbf{S}_{\text{C}_{4_j}}\big(\mathbf{W}, \mathbf{W}_\text{E}, \boldsymbol{\nu}, \boldsymbol{\beta}\big) \tag{1.20}$$

$$= \begin{bmatrix} \nu_j \mathbf{I}_{N_\text{T}N_\text{R}} & \mathbf{0} \\ \mathbf{0} & -\beta_j - \nu_j \upsilon_j^2 \end{bmatrix} + \mathbf{U}_{\widetilde{\mathbf{g}}_j}^H (\boldsymbol{\mathcal{W}} + \boldsymbol{\mathcal{W}}_\text{E}) \mathbf{U}_{\widetilde{\mathbf{g}}_j} \succeq \mathbf{0}, \forall j,$$

for $\boldsymbol{\nu} = \{\nu_1, \ldots, \nu_j, \ldots, \nu_J\}$, $\nu_j \geq 0$, $\boldsymbol{\mathcal{W}} = \mathbf{I}_{N_\text{R}} \otimes \mathbf{W}$, $\boldsymbol{\mathcal{W}}_\text{E} = \mathbf{I}_{N_\text{R}} \otimes \mathbf{W}_\text{E}$, $\mathbf{U}_{\widetilde{\mathbf{g}}_j} = [\mathbf{I}_{N_\text{T}N_\text{R}} \quad \widetilde{\mathbf{g}}_j]$, and $\widetilde{\mathbf{g}}_j = \text{vec}(\hat{\mathbf{G}}_j)$. Then, the considered optimization problem can be rewritten as

---

Problem 3 Rank-constrained SDP for SWIPT:

$$\underset{\mathbf{W},\mathbf{W}_\text{E} \in \mathbb{H}^{N_\text{T}}, \tau, \boldsymbol{\nu}, \delta, \boldsymbol{\beta}}{\text{maximize}} \quad \tau \tag{1.21}$$

subject to
$\text{C1}: \text{Tr}(\mathbf{W} + \mathbf{W}_\text{E}) \leq P_{\max}$,

$\text{C2}: M_j \geq \Theta_j\Big(1 + \exp\big(-a_j(\beta_j - b_j)\big)\Big), \forall j \in \{1, \ldots, J\}$,

$\text{C3}: \mathbf{S}_{\text{C}_3}\big(\mathbf{W}, \delta, \tau\big) \succeq \mathbf{0}$,

$\text{C4}: \mathbf{S}_{\text{C}_{4_j}}\big(\mathbf{W}, \mathbf{W}_\text{E}, \boldsymbol{\nu}, \boldsymbol{\beta}\big) \succeq \mathbf{0}, , \forall j \in \{1, \ldots, J\}$,

$\text{C5}: \text{Rank}(\mathbf{W}) \leq 1$,

$\text{C6}: \mathbf{W} \succeq \mathbf{0}$,

$\text{C7}: \mathbf{W}_\text{E} \succeq \mathbf{0}$,

where δ and $\boldsymbol{\nu}$ are the non-negative auxiliary optimization variables introduced in Lemma 1 for handling constraints C3 and C4, respectively. We note that constraints C3 and C4 involve only a finite number of LMI constraints which facilitates the resource allocation algorithm design. However, the rank constraint in C5 is still an obstacle in solving the considered optimization problem due to its combinatorial nature. As a result, we adopt SDP relaxation by removing constraint C5 from the problem formulation which yields:

Problem 4 SDP relaxation of (1.21)

$$\underset{\mathbf{W},\mathbf{W}_{\mathrm{E}}\in\mathbb{H}^{N_{\mathrm{T}}},\tau,\boldsymbol{\nu},\delta,\boldsymbol{\beta}}{\text{maximize}} \quad \tau \qquad\qquad\qquad\qquad\qquad\qquad\qquad\qquad (1.22)$$

$$\text{subject to} \quad \text{C1}: \ \mathrm{Tr}(\mathbf{W}+\mathbf{W}_{\mathrm{E}}) \leq P_{\max},$$

$$\text{C2}: \ M_j \geq \Theta_j\Big(1+\exp\big(-a_j(\beta_j-b_j)\big)\Big), \forall j \in \{1,\ldots,J\},$$

$$\text{C3}: \ \mathbf{S}_{\mathrm{C}_3}\big(\mathbf{W},\delta,\tau\big) \succeq \mathbf{0},$$

$$\text{C4}: \ \mathbf{S}_{\mathrm{C}_{4_j}}\big(\mathbf{W},\mathbf{W}_{\mathrm{E}},\boldsymbol{\nu},\boldsymbol{\beta}\big) \succeq \mathbf{0}, , \forall j \in \{1,\ldots,J\},$$

$$\text{C5}: \ \cancel{\underline{\mathrm{Rank}(\mathbf{W}) \leq 1}}.$$

$$\text{C6}: \ \mathbf{W} \succeq \mathbf{0},$$

$$\text{C7}: \ \mathbf{W}_{\mathrm{E}} \succeq \mathbf{0}\,.$$

The rank relaxed problem is a convex optimization problem and can be solved efficiently by standard numerical solvers such as CVX [49]. Yet, the constraint relaxation may not be tight when $\mathrm{Rank}(\mathbf{W}) > 1$ and in that case the result of the relaxed problem serves as a performance upper bound for the original problem. Therefore, we study the tightness of the adopted SDP relaxation in the following theorem.

Theorem 1 *Assuming the considered problem is feasible for $P_{\max} > 0$, a rank-one solution of* (1.22) *can always be constructed.*

Proof: Please refer to Appendix 1.6.1.

In other words, (1.21) can be solved optimally. In particular, information beamforming is optimal for the maximization of achievable rate, despite the imperfection of the CSI and non-linearity of the RF EH circuits.

1.3.6 Numerical Example

In this section, we evaluate the IoT system performance of the proposed optimal resource allocation algorithm via simulations. We summarize the important simulation parameters in Table 1.1. We assume that the IR and the J ERs are located at 100 meters and 5 meters from the transmitter, respectively. In particular, the IR is an IoT device connecting to the transmitter for information transfer while the J ERs are idle IoT receivers requesting wireless energy to extend their lifetimes. Unless further specified, we adopt the normalized maximum channel estimation errors of ER j and the IR as $\sigma^2_{\mathrm{est}_G} = 1\% \geq \frac{v_j^2}{\|\mathbf{G}_j\|_F^2}, \forall j$, and $\sigma^2_{\mathrm{est}_h} = 1\% \geq$

Table 1.1 Simulation Parameters.

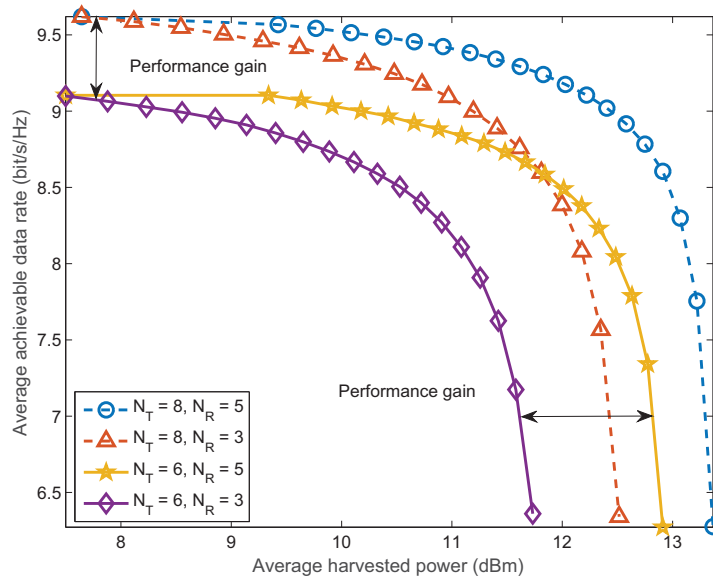| Carrier center frequency	915 MHz
Bandwidth	200 kHz
Transceiver antenna gain	10 dBi
Number of receive antennas N_{R}	2
Noise power σ^2	-95 dBm
Maximum transmit power $P_{\max}$	36 dBm
Transmitter-to-ER fading distribution	Rician with Rician factor 3 dB
Transmitter-to-IR fading distribution	Rayleigh

Figure 1.6 Average achievable data rate (bit/s/Hz) versus the average harvested power (dBm) for different numbers of antennas.

$\frac{\rho^2}{\|\mathbf{h}\|_2^2}$. For the non-linear EH circuits, we set $M_j = 24$ mW which corresponds to the maximum harvested power per wireless powered device. Besides, we adopt $a_j = 150$ and $b_j = 0.014$. We solve the optimization problem in (1.22) and obtain the average system performance by averaging over different channel realizations.

In Figure 1.6, we show the average achievable rate of the system versus the average total harvested energy in a downlink system for the optimal beamforming scheme. In particular, a transmitter equipped with N_{T} antennas serves a single-antenna IR and $J = 1$ ER. As can be observed, there is a non-trivial trade-off between the achievable system data rate and the total harvested energy. In other words, system data rate maximization and total harvested energy maximization are two conflicting system design objectives. Besides, for the optimal resource allocation, the trade-off region of the system achievable rate and the harvested energy is enlarged significantly with N_{T} and N_{R}. This is due to the fact that the extra degrees of freedom offered by multiple transmit antennas help the transmitter to focus the energy of the information signal and thus improve the beamforming efficiency. On the other hand, increasing the number of receive antennas N_{R} can significantly improve the total harvested
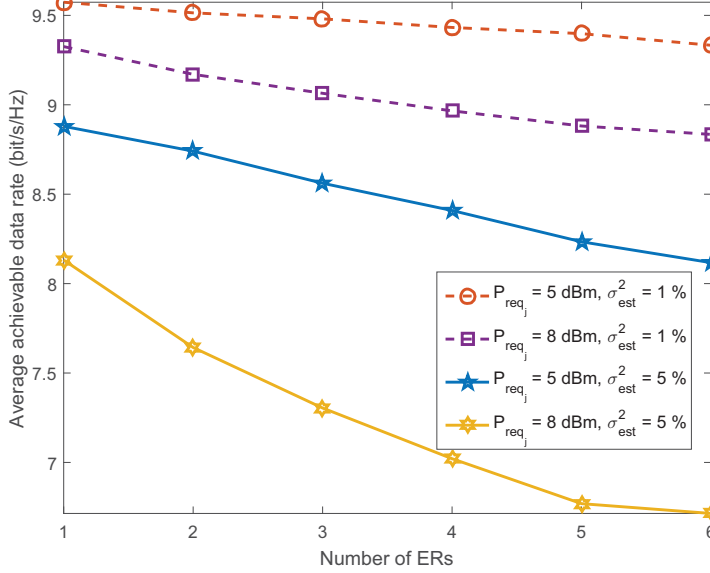
Figure 1.7 Average achievable data rate (bit/s/Hz) versus the number of ERs for $N_{\mathrm{T}} = 8$.

energy at the ER. In fact, the extra receiver antennas act as additional energy collectors which enables a more efficient energy transfer. Furthermore, it is verified by simulation that $\mathrm{Rank}(\mathbf{W}) = 1$ can be obtained/construsted for all the considered channel realizations which confirms the correctness of Theorem 1.

In Figure 1.7, we study the average achievable data rate versus the number of ERs for different maximum normalized channel estimation error variances. The maximum transmit power is $P_{\mathrm{max}} = 36$ dBm and $N_{\mathrm{R}} = 2$. Besides, the maximum normalized channel estimation error variance of the transmitter-to-IR link and the transmitter-to-ERs links are set to be identical, i.e., $\sigma^2_{\mathrm{est}_G} = \sigma^2_{\mathrm{est}_h} = \sigma^2_{\mathrm{est}}$. As can be observed, the average achievable data rate decreases with an increasing number of ERs. In fact, constraints C4 become more stringent when there are more ERs in the system which reduces the flexibility of the transmitter in resource allocation. In particular, for a large number of ERs in the system, the transmitter is forced to steer the transmit direction towards the ERs to improve the efficiency of wireless power transfer which reduces the received signal strength at the IR. On the other hand, the achievable data rate decreases with increasing σ^2_{est}, since the CSI quality degrades with increasing σ^2_{est}. In particular, for a larger value of σ^2_{est}, it becomes more difficult for the transmitter to focus the transmitter energy for improving the efficiency of SWIPT.

1.4 WIRELESS POWERED COMMUNICATION NETWORKS

In the last section, we studied the robust resource allocation algorithm design for systems where a transmitter provides information and wireless energy simultaneously to IR and ERs, respectively. In this section, we focus on a second line of research in WET: WPCN, where the wireless communication devices are first powered by WET and then use the harvested energy to transmit data. For instance, dedicated power beacons or power stations can be deployed in the system for WET. Compared to conventional base stations, power stations/beacons do not require data backhaul connections and can be installed in an ad-hoc or on-demand

manner. This kind of system setup has various IoT applications for energy-limited wireless communication sensors which need to first harvest enough energy from the environment before sending information to an information receiver. In the following, we discuss a resource allocation design to improve the system performance of such a WPCN.

1.4.1 Channel Model

A simple WPCN is considered in this section. We assume that there is a power station transferring wireless energy to J wireless powered mobile users in the downlink to facilitate their information transfer in the uplink, cf. Figure 1.8. We assume that both the power station and each of the wireless powered mobile user are equipped with $N_{\mathrm{T}} > 1$ and $N_{\mathrm{R}} > 1$ antennas, respectively, to facilitate efficient energy and information transfer. On the other hand, there is a single-antenna IR receiving the uplink information from the J wireless powered mobile users. In the considered network, we adopt the "harvest-then-transmit" protocol [12, 50, 51] for WET and information transmission. Specifically, the transmission is divided into two orthogonal time periods, namely the WET period and wireless information transfer (WIT) period, cf. Figure 1.9. In the WET period, the power station sends an energy signal to the J wireless powered users for EH. The instantaneous received signal at mobile user $j \in \{1, \ldots, J\}$ is given by

$$\mathbf{y}_{\mathrm{EH}_j} = \mathbf{G}_j^H \mathbf{v} + \mathbf{n}_{\mathrm{EH}_j}, \tag{1.23}$$

where $\mathbf{v} \in \mathbb{C}^{N_{\mathrm{T}} \times 1}$ is the beamforming vector in the downlink for WET. The channel matrix between the power station and mobile user j is denoted by $\mathbf{G}_j \in \mathbb{C}^{N_{\mathrm{T}} \times N_{\mathrm{R}}}$. Vector $\mathbf{n}_{\mathrm{EH}_j} \sim \mathcal{CN}(\mathbf{0}, \sigma_{\mathrm{s}_j}^2 \mathbf{I}_{N_{\mathrm{R}}})$ is the AWGN at mobile user j. Then, in the WIT period, the J wireless powered mobile users exploit the energy harvested in the RF to transmit independent information signals in the uplink to the information receiver in a time division manner. In particular, mobile user J is allocated τ_j amount of time for uplink transmission. The instantaneous received signal at the information receiver from mobile user j is given by

$$y_j^{\mathrm{IR}} = \mathbf{h}_j^H \mathbf{w}_j s_j + n, \ \forall j \in \{1, \ldots, J\}, \tag{1.24}$$

where $\mathbf{h}_j \in \mathbb{C}^{N_{\mathrm{R}} \times 1}$ is the channel vector between wireless powered user j and the information receiver. Scalar $s_j \in \mathbb{C}$ is the information signal of mobile user j, $\mathbf{w}_j \in \mathbb{C}^{N_{\mathrm{R}} \times 1}$ is the precoding vector adopted by user j intended for WIT, and $n \sim \mathcal{CN}(0, \sigma_{\mathrm{n}}^2)$ is the AWGN at the information receiver. Without loss of generality, we assume that $\mathcal{E}\{|s_j|^2\} = 1, \forall j \in \{1, \ldots, J\}$.

Channel State Information

In practice, a power station is expected to be a simple device with limited signal processing capability. As a result, the estimates of the CSI of the communication links between the power station and the J wireless powered users may not be perfect. To capture the imperfectness of the CSI for resource allocation, we adopt equations (1.10) and (1.11). In contrast, a sophisticated information receiver can be implemented in WPCNs for signal processing. Therefore, we assume that the CSI of the communication links between the the J wireless powered users and the information receiver is perfectly known for resource allocation design.

1.4.2 Problem Formulation and Solution

The resource allocation policy, $\{\boldsymbol{\tau}, \mathbf{V}, \mathbf{w}_j\}$, for maximizing the total system throughput can be obtained by solving the following problem:
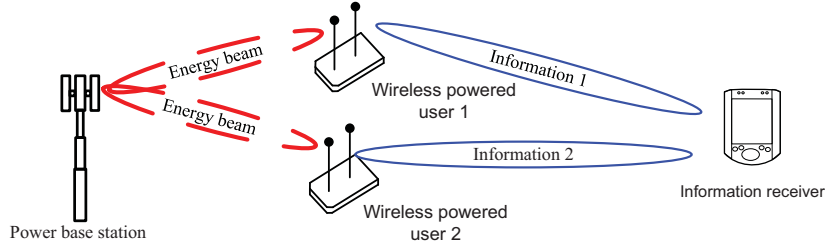
Figure 1.8 A WPCN with $J = 2$ multiple-antenna wireless powered users harvesting energy from a dedicated power base station. The harvested energy will be exploited for future information transmission.
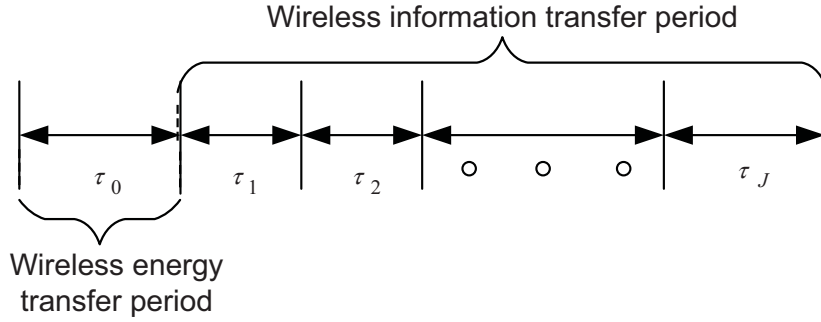

Figure 1.9 Wireless energy and information transfer protocol.

Problem 5 Robust Resource Allocation for WPCN:

$$\underset{\mathbf{V}\in\mathbb{H}^{N_{\mathrm{T}}},\mathbf{w}_j,\tau_j}{\text{maximize}} \quad \sum_{j=1}^{J}\tau_j\log_2\left(1+\frac{|\mathbf{h}_j^H\mathbf{w}_j|^2}{\sigma_{\mathrm{s}}^2}\right) \tag{1.25}$$

subject to   C1 : $\mathrm{Tr}(\mathbf{V}) \leq P_{\max}$,

C2 : $\tau_0 + \sum_{j=1}^{J}\tau_j \leq T_{\max}$,

C3 : $\tau_j\|\mathbf{w}_j\|^2 \leq \underset{\Delta\mathbf{G}_j\in\mathbf{\Xi}_j}{\min}\ \tau_0\dfrac{\dfrac{M_j}{1+\exp\left(-a_j(\mathrm{Tr}(\mathbf{V}\mathbf{G}_j\mathbf{G}_j^H)-b_j)\right)}-M_j\Omega_j}{1-\Omega_j},\ \forall j,$

C4 : $\tau_r \geq 0, \forall r \in \{0,1,\ldots,J\}$,

C5 : $\mathbf{V} \succeq \mathbf{0}$.

Constants $P_{\max}$ and $T_{\max}$ in constraints C1 and C2 are the maximum transmit power for the power station and the maximum duration of a time slot, respectively. Constraint C3 is imposed such that for a given CSI uncertainty set $\mathbf{\Xi}_j$, the maximum energy available for information transmission at wireless powered user j is limited by the total harvested RF energy during the wireless EH period τ_j. In particular, the right-hand side of constraint C3

denotes the total harvested power at ER j if a practical non-linear RF EH circuit is assumed[2]. C4 is the non-negativity constraint for information scheduling variable τ_j. Constraint C5 and $\mathbf{V} \in \mathbb{H}^{N_\mathrm{T}}$ constrain matrix $\mathbf{V}$ to be a positive semi-definite Hermitian matrix.

The optimization problem in (1.25) is a non-convex optimization problem which involves infinitely many constraints in C3. Besides, inequality constraint C3 involves the coupling of optimization variables τ_j and $\mathbf{w}_j$. Furthermore, the right-hand side of constraint C3 is a quasi-concave function. In general, there is no systematic approach for solving non-convex optimization problems. In order to obtain a computationally efficient resource allocation algorithm design, we introduce several transformations of the optimization problem. First, to handle the quasi-concavity of constraint C3, we solve the optimization problem for a fixed constant τ_0 and obtain an optimal solution for one instant of the optimization problem. Then, we repeat the procedure for all possible values of τ_0 and record the corresponding achieved system objective values. At the end, we select that τ_0 as the optimal time allocation for WET from all the trials which provides the maximum system objective value. Therefore, in the sequel, we assume that τ_0 is given by its optimal value for the design of the resource allocation algorithm.

Next, we introduce a change of variable to decouple the optimization variables in constraint C3. Specifically, we define a new optimization variable $\tilde{\mathbf{w}}_j = \sqrt{\tau}_j \mathbf{w}_j$ and rewrite the optimization problem as

---

Problem 6 Transformed Problem for WPCN:

$$\underset{\mathbf{V} \in \mathbb{H}^{N_\mathrm{T}}, \tilde{\mathbf{w}}_j \in \mathbb{H}^{N_\mathrm{U}}, \tau_j, \beta_j}{\text{maximize}} \quad \sum_{j=1}^{J} \tau_j \log_2 \left(1 + \frac{|\mathbf{h}_j^H \tilde{\mathbf{w}}_j|^2}{\tau_j \sigma_\mathrm{s}^2} \right) \tag{1.26}$$

$$\text{subject to} \quad \mathrm{C1}: \ \mathrm{Tr}(\mathbf{V}) \leq P_{\max},$$

$$\mathrm{C2}: \ \tau_0 + \sum_{j=1}^{J} \tau_j \leq T_{\max},$$

$$\mathrm{C3}: \ \|\tilde{\mathbf{w}}_j\|^2 \leq \tau_0 \frac{\frac{M_j}{1 + \exp\left(-a_j(\beta_j - b_j) \right)} - M_j \Omega_j}{1 - \Omega_j}, \ \forall j,$$

$$\mathrm{C4}: \ \tau_r \geq 0, \forall r \in \{0, 1, \ldots, J\},$$

$$\mathrm{C5}: \ \mathbf{V} \succeq \mathbf{0},$$

$$\mathrm{C6}: \ \min_{\Delta \mathbf{G}_j \in \boldsymbol{\Xi}_j} \mathrm{Tr}(\mathbf{V} \mathbf{G}_j \mathbf{G}_j^H) \geq \beta_j, \forall j \in \{1, \ldots, J\}.$$

To handle the infinitely many constraints in C6, we can apply Lemma 1 for (1.26). In particular, constraint C6 can be equivalently written as

$$\mathrm{C6}: \mathbf{S}_{\mathrm{C}6_j}\left(\mathbf{V}, \boldsymbol{\mu}, \boldsymbol{\beta}\right) \tag{1.27}$$

$$= \begin{bmatrix} \nu_j \mathbf{I}_{N_\mathrm{T} N_\mathrm{R}} & \mathbf{0} \\ \mathbf{0} & -\beta_j - \nu_j \upsilon_j^2 \end{bmatrix} + \mathbf{U}_{\tilde{\mathbf{g}}_j}^H \boldsymbol{\mathcal{V}} \mathbf{U}_{\tilde{\mathbf{g}}_j} \succeq \mathbf{0}, \forall j,$$

for $\boldsymbol{\nu} = \{\nu_1, \ldots, \nu_j, \ldots, \nu_J\}$, $\nu_j \geq 0$, $\boldsymbol{\mathcal{V}} = \mathbf{I}_{N_\mathrm{R}} \otimes \mathbf{V}$, $\mathbf{U}_{\tilde{\mathbf{g}}_j} = [\mathbf{I}_{N_\mathrm{T} N_\mathrm{R}} \quad \tilde{\mathbf{g}}_j]$, and $\tilde{\mathbf{g}}_j = \mathrm{vec}(\hat{\mathbf{G}}_j)$.

---

[2]Here, we assume that the circuit power consumption of each wireless powered user is negligibly small compared to the transmit power consumption and thus is not taken into account.

Table 1.2 Simulation Parameters.

Carrier center frequency	915 MHz
Bandwidth	200 kHz
Transceiver antenna gain	10 dBi
Noise power (including quantization noise) σ^2	-47 dBm
Power station-to-wireless powered user distance	5 meters
Power station-to-wireless powered user fading distribution	Rician with Rician factor 3 dB
Wireless powered user-to-IR fading distribution	Rayleigh
Maximum duration of a communication slot, $T_{\max}$	1 unit

Problem 7 Transformed Problem for WPCN:

$$\underset{\mathbf{V}\in\mathbb{H}^{N_{\mathrm{T}}},\tilde{\mathbf{w}}_j\in\mathbb{H}^{N_{\mathrm{U}}},\tau_j,\beta_j,\mu_j}{\text{maximize}} \quad \sum_{j=1}^{J}\tau_j\log_2\left(1+\frac{|\mathbf{h}_j^H\tilde{\mathbf{w}}_j|^2}{\tau_j\sigma_{\mathrm{s}}^2}\right) \tag{1.28}$$

$$\text{subject to} \quad \mathrm{C1-C5},$$

$$\mathrm{C6}: \ \mathbf{S}_{\mathrm{C}_{6_j}}\left(\mathbf{V},\boldsymbol{\mu},\boldsymbol{\beta}\right)\succeq\mathbf{0},\forall j\in\{1,\ldots,J\}.$$

The above transformed problem is jointly concave with respect to the optimization variables and can be solved efficiently via standard numerical solvers for convex programs.

1.4.3 Numerical Example

In this section, we evaluate the IoT system performance of the proposed resource allocation algorithm via simulations. We summarize the relevant simulation parameters in Table 1.2. We assume that a dedicated power station is deployed for wireless charging of IoT devices. There are $J=4$ ERs in the IoT network requiring energy for WIT. For the non-linear EH circuits, we set $M_j=24$ mW which corresponds to the maximum harvested power per ER. Besides, we adopt $a_j=150$ and $b_j=0.014$. To obtain the average system performance, we solve the optimization problem in (1.28) for each channel realization and average the result over different channel realizations.

In Figure 1.10, we study the average total system throughput versus the maximum transmit power from the power station, $P_{\max}$, for different numbers of antennas equipped at the power station, N_{T}, and at the wireless powered users, N_{R}. We set the normalized maximum channel estimation errors of wireless powered user j as $\sigma_{\mathrm{est}_G}^2=1\%\geq\frac{v_j^2}{\|\mathbf{G}_j\|_F^2},\forall j$. As can be observed, the average total system throughput increases with increasing $P_{\max}$. Indeed, with a higher value of $P_{\max}$, the wireless powered users are able to harvest more energy for information transmission. However, there is a diminishing return in performance as $P_{\max}$ increases in the high transmit power regime. This is due to the fact that the high transmit power from the power station causes saturation in practical non-linear EH circuits which limits the available harvested power for WIT. On the other hand, when the number of antennas equipped at the power base station increases, a higher system throughput can be achieved by the proposed optimal scheme. In fact, the extra antennas provide extra spatial degrees of freedom which facilitates a more flexible resource allocation, since the power station can steer the energy signal towards the wireless powered users more accurately to improve the efficiency of WET.
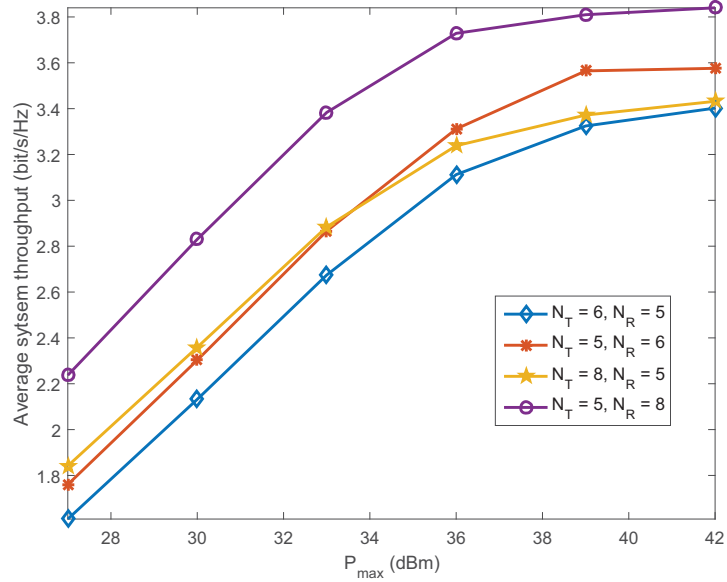
Figure 1.10 Average system throughput (bit/s/Hz) versus the maximum transmit power at the power base station (dBm).
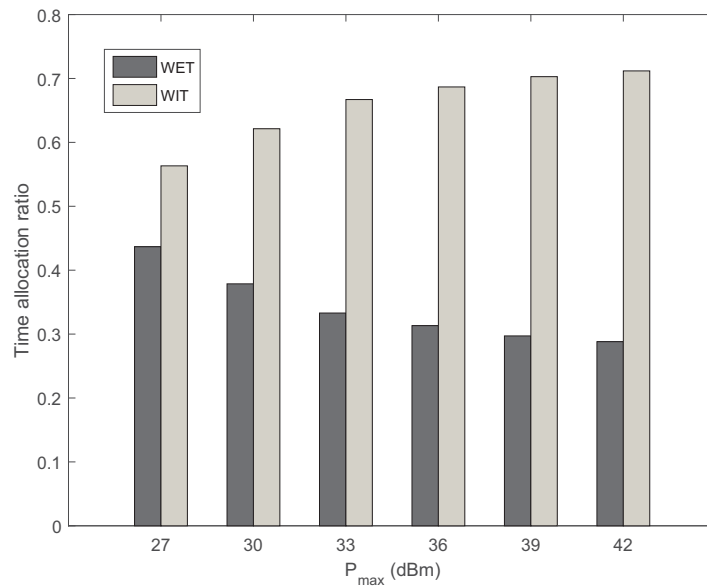

Figure 1.11 Time allocation ratio for WET and WIT versus the maximum transmit power at the power base station (dBm).

Besides, the system throughput increases rapidly with the number of antennas equipped at the wireless powered users. In fact, the extra antennas equipped at the wireless powered users act as additional wireless energy collectors which increase the amount of total harvested energy. Furthermore, the extra antennas at the wireless powered users would also provide extra spatial degrees of freedom which improves the transmit beamforming gain in the WIT phase.

Figure 1.11 shows the time allocation ratio for the proposed algorithm with respect to the WET and WIT periods for the case of $N_{\mathrm{T}} = 6$ and $N_{\mathrm{R}} = 5$ in Figure 1.10. As can be observed, WET period for the proposed scheme becomes shorter as the value of $P_{\max}$ increases. In fact, for a higher maximum transmit power from the power station, the wireless powered users can harvest the amount of energy required for information transmission in a shorter period of time. In contrast, the WIT period becomes longer for an increasing value of $P_{\max}$. This is due to the fact that the achievable throughput of each wireless powered user is an increasing function with respect to the time allocation for information transmission, i.e., τ_j, for a fixed amount of total transmit energy. In the extreme case, for a sufficiently large $P_{\max}$, one can expect that $\tau_0 \to 0$ since an infinitesimal amount of time is enough to provide sufficient energy to fully charge the wireless powered users.

1.5 CONCLUSION

In this chapter, we studied resource allocation algorithms for two RF-based EH wireless communication network architectures, which are of interest for IoT applications. We first discussed a parametric non-linear EH model which facilitates the resource allocation algorithm design to enable efficient wireless powered IoT communication networks. The algorithm designs were formulated as two non-convex optimization problems for maximizing the sum-throughput in SWIPT and WPCN systems, respectively. The problem formulations took into account the imperfectness of the CSI and the non-linearity of the EH circuits in order to ensure robust resource allocation. The proposed resource allocation design optimization problems were optimally solved by advanced signal processing techniques. Numerical results showed the potential gains in harvested power enabled by the proposed optimization and the benefits in adopting multiple-antenna technology for IoT communication networks.

1.6 APPENDIX

1.6.1 Proof of Theorem 1

We provide a method for constructing an optimal rank-one solution for (1.22) when Rank($\mathbf{W}$) > 1 is obtained from (1.22). For a given optimal τ^* from the solution of (1.22), we solve the following auxiliary convex optimization problem [52, 53]:

Auxiliary Convex Optimization Problem

$$\underset{\mathbf{W},\mathbf{W}_\mathrm{E}\in\mathbb{H}^{N_\mathrm{T}},\,\boldsymbol{\nu},\delta,\boldsymbol{\beta}}{\text{minimize}} \quad \text{Tr}(\mathbf{W}) \tag{1.29}$$

$$\text{subject to} \quad \mathrm{C1},\mathrm{C2},\mathrm{C4},\mathrm{C6},\mathrm{C7},$$

$$\mathrm{C3}:\ \mathbf{S}_{\mathrm{C}_3}\Big(\mathbf{W},\delta,\tau^*\Big)\succeq\mathbf{0}\,.$$

We note that the optimal resource allocation policy obtained from the above auxiliary convex optimization problem is also an optimal resource allocation policy for (1.22), since both problems have the same feasible solution set and τ^* is fixed for (1.29).

Now, we aim to show that (1.29) admits a rank-one beamforming matrix. In this context, we first need the Lagrangian of problem (1.29):

$$\begin{aligned}
L &= \text{Tr}(\mathbf{W}) + \lambda(\text{Tr}(\mathbf{W} + \mathbf{W}_\mathrm{E}) - P_{\max}) - \text{Tr}(\mathbf{W}\mathbf{Y}) \\
&\quad - \sum_{j=1}^{J} \text{Tr}(\mathbf{S}_{\mathrm{C}_{4_j}}\Big(\mathbf{W},\mathbf{W}_\mathrm{E},\boldsymbol{\nu},\boldsymbol{\beta}\Big)\mathbf{D}_{\mathrm{C}_{4_j}}) \\
&\quad - \text{Tr}(\mathbf{S}_{\mathrm{C}_3}\Big(\mathbf{W},\delta,\tau\Big)\mathbf{D}_{\mathrm{C}_3}) - \text{Tr}(\mathbf{W}_\mathrm{E}\mathbf{Z}) + \boldsymbol{\Delta},
\end{aligned} \tag{1.30}$$

where $\lambda \geq 0$, $\mathbf{D}_{\mathrm{C}_3} \succeq \mathbf{0}$, $\mathbf{D}_{\mathrm{C}_{4_j}} \succeq \mathbf{0}, \forall j \in \{1,\ldots,J\}$, $\mathbf{Y} \succeq \mathbf{0}$, and $\mathbf{Z} \succeq \mathbf{0}$ are the dual variables for constraints C1, C3, C4, C6, and C7, respectively. $\boldsymbol{\Delta}$ is a collection of primal and dual variables and constants that are not relevant to the proof.

Now, we focus on those Karush-Kuhn-Tucker (KKT) conditions which are needed for the proof.

KKT conditions:

$$\mathbf{Y}^*, \mathbf{Z}^*, \mathbf{D}^*_{\mathrm{C}_3}, \mathbf{D}^*_{\mathrm{C}_{4_j}} \succeq \mathbf{0}, \quad \lambda^* \geq 0, \tag{1.31a}$$

$$\mathbf{Y}^*\mathbf{W}^* = \mathbf{0}, \quad \mathbf{Q}^*\mathbf{V}^* = \mathbf{0}, \tag{1.31b}$$

$$\mathbf{Y}^* = (1 + \lambda^*)\mathbf{I}_{N_\mathrm{T}} - \mathbf{U}_{\hat{\mathbf{h}}}\mathbf{D}_{\mathrm{C}_2}\mathbf{U}_{\hat{\mathbf{h}}}^H - \boldsymbol{\Xi}, \tag{1.31c}$$

$$\mathbf{Z}^* = \lambda^*\mathbf{I}_{N_\mathrm{T}} - \boldsymbol{\Xi}, \tag{1.31d}$$

$$\mathbf{S}_{\mathrm{C}_3}\Big(\mathbf{W},\delta,\tau\Big)\mathbf{D}_{\mathrm{C}_3} = \mathbf{0}, \tag{1.31e}$$

---

where $\boldsymbol{\Xi} = \sum_{j=1}^{J}\sum_{l=1}^{N_\mathrm{R}}\Big[\mathbf{U}_{\widetilde{\mathbf{g}}_j}\mathbf{D}_{\mathrm{C}_{4_j}}\mathbf{U}_{\widetilde{\mathbf{g}}_j}^H\Big]_{a:b,c:d}, a = (l-1)N_\mathrm{T} + 1, b = lN_\mathrm{T}, c = (l-1)N_\mathrm{T} + 1,$ and $d = lN_\mathrm{T}$. The optimal primal and dual variables of the SDP relaxed version are denoted by the corresponding variables with an asterisk superscript.

Subtracting (1.31d) from (1.31c) yields:

$$\mathbf{Y}^* + \mathbf{U}_{\hat{\mathbf{h}}}\mathbf{D}_{\mathrm{C}_3}\mathbf{U}_{\hat{\mathbf{h}}}^H = \mathbf{Z}^* + \mathbf{I}_{N_\mathrm{T}}. \tag{1.32}$$

Next, we multiply the both sides of (1.31c) by $\mathbf{W}^*$ leading to

$$\mathbf{W}^* \mathbf{U}_{\hat{\mathbf{h}}} \mathbf{D}_{C_3} \mathbf{U}_{\hat{\mathbf{h}}}^H = \mathbf{W}^*(\mathbf{Z}^* + \mathbf{I}_{N_T}). \tag{1.33}$$

From (1.33), we can deduce that

$$\begin{aligned}
\mathrm{Rank}(\mathbf{W}^*) &= \mathrm{Rank}(\mathbf{W}^* \mathbf{U}_{\hat{\mathbf{h}}} \mathbf{D}_{C_3} \mathbf{U}_{\hat{\mathbf{h}}}^H) \\
&\leq \min\{\mathrm{Rank}(\mathbf{W}^*), \mathrm{Rank}(\mathbf{U}_{\hat{\mathbf{h}}} \mathbf{D}_{C_3} \mathbf{U}_{\hat{\mathbf{h}}}^H)\}.
\end{aligned} \tag{1.34}$$

Therefore, if $\mathrm{Rank}(\mathbf{U}_{\hat{\mathbf{h}}} \mathbf{D}_{C_3} \mathbf{U}_{\hat{\mathbf{h}}}^H) \leq 1$, then $\mathrm{Rank}(\mathbf{W}^*) \leq 1$. To show $\mathrm{Rank}(\mathbf{U}_{\hat{\mathbf{h}}} \mathbf{D}_{C_3} \mathbf{U}_{\hat{\mathbf{h}}}^H) \leq 1$, we pre-multiply and post-multiply (1.31e) by $[\mathbf{I}_{N_T} \ \mathbf{0}]$ and $\mathbf{U}_{\hat{\mathbf{h}}}^H$, respectively. After some mathematical manipulations, we have the following equality:

$$(\delta \mathbf{I}_{N_T} + \mathbf{W}^*) \mathbf{U}_{\hat{\mathbf{h}}} \mathbf{D}_{C_3} \mathbf{U}_{\hat{\mathbf{h}}}^H = \delta [\mathbf{0} \ \hat{\mathbf{h}}] \mathbf{D}_{C_3} \mathbf{U}_{\hat{\mathbf{h}}}^H. \tag{1.35}$$

Besides, it can be shown that $\delta \mathbf{I}_{N_T} + \mathbf{W}^* \succ \mathbf{0}$ and $\delta > 0$ hold for the optimal solution such that the dual optimal solution is bounded from above. Therefore, we have

$$\mathrm{Rank}(\mathbf{U}_{\hat{\mathbf{h}}} \mathbf{D}_{C_3} \mathbf{U}_{\hat{\mathbf{h}}}^H) = \mathrm{Rank}(\delta [\mathbf{0} \ \hat{\mathbf{h}}] \mathbf{D}_{C_3} \mathbf{U}_{\hat{\mathbf{h}}}^H) \leq \mathrm{Rank}([\mathbf{0} \ \hat{\mathbf{h}}]) \leq 1. \tag{1.36}$$

By combining (1.34) and (1.36), we can conclude that $\mathrm{Rank}(\mathbf{W}^*) \leq 1$. On the other hand, $\mathbf{W}^* \neq \mathbf{0}$ is not optimal for $P_{\max} > 0$ and thus $\mathrm{Rank}(\mathbf{W}^*) = 1$. ■

Bibliography

[1] M. Zorzi, A. Gluhak, S. Lange, and A. Bassi, "From today's INTRAnet of things to a Future INTERnet of Things: a Wireless- and Mobility-Related View," *IEEE Wireless Commun.*, vol. 17, pp. 44–51, Dec. 2010.

[2] D. W. K. Ng, E. S. Lo, and R. Schober, "Energy-Efficient Resource Allocation in OFDMA Systems with Hybrid Energy Harvesting Base Station," *IEEE Trans. Wireless Commun.*, vol. 12, pp. 3412–3427, Jul. 2013.

[3] M. Zhang and Y. Liu, "Energy Harvesting for Physical-Layer Security in OFDMA Networks," *IEEE Trans. Inf. Forensics Security*, vol. 11, pp. 154–162, Jan. 2016.

[4] I. Ahmed, A. Ikhlef, D. W. K. Ng, and R. Schober, "Power Allocation for an Energy Harvesting Transmitter with Hybrid Energy Sources," *IEEE Trans. Wireless Commun.*, vol. 12, pp. 6255–6267, Dec. 2013.

[5] P. Grover and A. Sahai, "Shannon Meets Tesla: Wireless Information and Power Transfer," in *Proc. IEEE Intern. Sympos. on Inf. Theory*, Jun. 2010, pp. 2363 –2367.

[6] I. Krikidis, S. Timotheou, S. Nikolaou, G. Zheng, D. W. K. Ng, and R. Schober, "Simultaneous Wireless Information and Power Transfer in Modern Communication Systems," *IEEE Commun. Mag.*, vol. 52, no. 11, pp. 104–110, Nov. 2014.

[7] Z. Ding, C. Zhong, D. W. K. Ng, M. Peng, H. A. Suraweera, R. Schober, and H. V. Poor, "Application of Smart Antenna Technologies in Simultaneous Wireless Information and Power Transfer," *IEEE Commun. Mag.*, vol. 53, no. 4, pp. 86–93, Apr. 2015.

[8] X. Chen, Z. Zhang, H.-H. Chen, and H. Zhang, "Enhancing Wireless Information and Power Transfer by Exploiting Multi-Antenna Techniques," *IEEE Commun. Mag.*, no. 4, pp. 133–141, Apr. 2015.

[9] X. Chen, D. W. K. Ng, and H.-H. Chen, "Secrecy Wireless Information and Power Transfer: Challenges and Opportunities," *IEEE Commun. Mag.*, vol. 23, no. 2, pp. 54–61, Apr. 2016.

[10] X. Chen, J. Chen, and T. Liu, "Secure Transmission in Wireless Powered Massive MIMO Relaying Systems: Performance Analysis and Optimization," *to appear in IEEE Trans. Veh. Technol.*, 2016.

[11] C. Zhong, X. Chen, Z. Zhang, and G. K. Karagiannidis, "Wireless-Powered Communications: Performance Analysis and Optimization," *IEEE Trans. Commun.*, vol. 63, pp. 5178–5190, Dec. 2015.

[12] Q. Wu, M. Tao, D. Ng, W. Chen, and R. Schober, "Energy-Efficient Resource Allocation for Wireless Powered Communication Networks," *IEEE Trans. Wireless Commun.*, vol. 15, pp. 2312–2327, Mar. 2016.

[13] X. Chen, X. Wang, and X. Chen, "Energy-Efficient Optimization for Wireless Information and Power Transfer in Large-Scale MIMO Systems Employing Energy Beamforming," *IEEE Wireless Commun. Lett.*, vol. 2, pp. 1–4, Dec. 2013.

[14] D. W. K. Ng, E. S. Lo, and R. Schober, "Wireless Information and Power Transfer: Energy Efficiency Optimization in OFDMA Systems," *IEEE Trans. Wireless Commun.*, vol. 12, pp. 6352–6370, Dec. 2013.

[15] M. Zhang, Y. Liu, and R. Zhang, "Artificial Noise Aided Secrecy Information and Power Transfer in OFDMA Systems," *IEEE Trans. Wireless Commun.*, vol. 15, pp. 3085–3096, Apr. 2016.

[16] Y. Liu, "Wireless Information and Power Transfer for Multirelay-Assisted Cooperative Communication," vol. 20, pp. 784–787, Apr. 2016.

[17] R. Zhang and C. K. Ho, "MIMO Broadcasting for Simultaneous Wireless Information and Power Transfer," *IEEE Trans. Wireless Commun.*, vol. 12, pp. 1989–2001, May 2013.

[18] S. Leng, D. W. K. Ng, N. Zlatanov, and R. Schober, "Multi-Objective Resource Allocation in Full-Duplex SWIPT Systems," in *Proc. IEEE Intern. Commun. Conf.*, May 2016.

[19] D. W. K. Ng, E. S. Lo, and R. Schober, "Robust Beamforming for Secure Communication in Systems with Wireless Information and Power Transfer," *IEEE Trans. Wireless Commun.*, vol. 13, pp. 4599–4615, Aug. 2014.

[20] D. W. K. Ng and R. Schober, "Secure and Green SWIPT in Distributed Antenna Networks with Limited Backhaul Capacity," *IEEE Trans. Wireless Commun.*, vol. 14, no. 9, pp. 5082–5097, Sep. 2015.

[21] M. Khandaker and K.-K. Wong, "Robust Secrecy Beamforming With Energy-Harvesting Eavesdroppers," *IEEE Wireless Commun. Lett.*, vol. 4, pp. 10–13, Feb. 2015.

[22] D. W. K. Ng, E. S. Lo, and R. Schober, "MultiObjective Resource Allocation for Secure Communication in Cognitive Radio Networks with Wireless Information and Power Transfer," *IEEE Trans. Veh. Technol.*, vol. 65, pp. 3166–3184, May 2016.

[23] Q. Wu, W. Chen, and J. Li, "Wireless Powered Communications With Initial Energy: QoS Guaranteed Energy-Efficient Resource Allocation," *IEEE Wireless Commun. Lett.*, vol. 19, pp. 2278–2281, Dec. 2015.

[24] E. Boshkovska, D. Ng, N. Zlatanov, and R. Schober, "Practical Non-Linear Energy Harvesting Model and Resource Allocation for SWIPT Systems," *IEEE Commun. Lett.*, vol. 19, pp. 2082–2085, Dec. 2015.

[25] S. Kisseleff, I. F. Akyildiz, and W. Gerstacker, "Beamforming for Magnetic Induction Based Wireless Power Transfer Systems with Multiple Receivers," in *Proc. IEEE Global Telecommun. Conf.*, Dec. 2015, pp. 1–7.

[26] S. Kisseleff, X. Chen, I. F. Akyildiz, and W. Gerstacker, "Wireless Power Transfer for Access Limited Wireless Underground Sensor Networks," in *Proc. IEEE Intern. Commun. Conf.*, May 2016.

[27] S. Kisseleff, X. Chen, I. F. Akyildiz, and W. H. Gerstacker, "Efficient Charging of Access Limited Wireless Underground Sensor Networks," *IEEE Trans. Commun.*, vol. 64, no. 5, pp. 2130–2142, May 2016.

[28] Powercast Coporation, "RF Energy Harvesting and Wireless Power for Low-Power Applications," 2011. [Online]. Available: http://www.mouser.com/pdfdocs/Powercast-Overview-2011-01-25.pdf

[29] D. W. K. Ng, E. S. Lo, and R. Schober, "Energy-Efficient Resource Allocation in Multi-Cell OFDMA Systems with Limited Backhaul Capacity," *IEEE Trans. Wireless Commun.*, vol. 11, pp. 3618–3631, Oct. 2012.

[30] D. W. K. Ng, E. Lo, and R. Schober, "Energy-Efficient Resource Allocation in OFDMA Systems with Large Numbers of Base Station Antennas," *IEEE Trans. Wireless Commun.*, vol. 11, pp. 3292 –3304, Sep. 2012.

[31] Q. Wu, W. Chen, M. Tao, J. Li, H. Tang, and J. Wu, "Resource Allocation for Joint Transmitter and Receiver Energy Efficiency Maximization in Downlink OFDMA Systems," *IEEE Trans. Commun.*, vol. 63, pp. 416–430, Feb. 2015.

[32] Q. Wu, M. Tao, and W. Chen, "Joint Tx/Rx Energy-Efficient Scheduling in Multi-Radio Wireless Networks: A Divide-and-Conquer Approach," *IEEE Trans. Wireless Commun.*, vol. 15, pp. 2727–2740, Apr. 2016.

[33] L. Varshney, "Transporting Information and Energy Simultaneously," in *Proc. IEEE Intern. Sympos. on Inf. Theory*, Jul. 2008, pp. 1612 –1616.

[34] C. W. Lander, *Power Electronics: Principles and Practice.* McGraw-Hill, 1993, vol. 3rd ed.

[35] C. Valenta and G. Durgin, "Harvesting Wireless Power: Survey of Energy-Harvester Conversion Efficiency in Far-Field, Wireless Power Transfer Systems," *IEEE Microw. Mag.*, vol. 15, pp. 108–120, Jun. 2014.

[36] X. Zhou, R. Zhang, and C. K. Ho, "Wireless Information and Power Transfer: Architecture Design and Rate-Energy Tradeoff," in *Proc. IEEE Global Telecommun. Conf.*, Dec. 2012.

[37] D. W. K. Ng, E. S. Lo, and R. Schober, "Energy-Efficient Resource Allocation in Multiuser OFDM Systems with Wireless Information and Power Transfer," in *Proc. IEEE Wireless Commun. and Netw. Conf.*, 2013.

[38] S. Leng, D. W. K. Ng, and R. Schober, "Power Efficient and Secure Multiuser Communication Systems with Wireless Information and Power Transfer," in *Proc. IEEE Intern. Commun. Conf.*, Jun. 2014.

[39] D. W. K. Ng, L. Xiang, and R. Schober, "Multi-Objective Beamforming for Secure Communication in Systems with Wireless Information and Power Transfer," in *Proc. IEEE Personal, Indoor and Mobile Radio Commun. Sympos.*, Sep. 2013.

[40] D. W. K. Ng, R. Schober, and H. Alnuweiri, "Secure Layered Transmission in Multicast Systems With Wireless Information and Power Transfer," in *Proc. IEEE Intern. Commun. Conf.*, Jun. 2014, pp. 5389–5395.

[41] D. W. K. Ng and R. Schober, "Resource Allocation for Coordinated Multipoint Networks With Wireless Information and Power Transfer," in *Proc. IEEE Global Telecommun. Conf.*, Dec. 2014, pp. 4281–4287.

[42] M. Chynonova, R. Morsi, D. W. K. Ng, and R. Schober, "Optimal Multiuser Scheduling Schemes for Simultaneous Wireless Information and Power Transfer," in *23rd European Signal Process. Conf. (EUSIPCO)*, Aug. 2015.

[43] Q. Wu, M. Tao, D. W. K. Ng, W. Chen, and R. Schober, "Energy-Efficient Transmission for Wireless Powered Multiuser Communication Networks," in *Proc. IEEE Intern. Commun. Conf.*, Jun. 2015.

[44] D. Ng and R. Schober, "Max-Min Fair Wireless Energy Transfer for Secure Multiuser Communication Systems," in *IEEE Inf. Theory Workshop (ITW)*, Nov. 2014, pp. 326–330.

[45] J. Guo and X. Zhu, "An Improved Analytical Model for RF-DC Conversion Efficiency in Microwave Rectifiers," in *IEEE MTT-S Int. Microw. Symp. Dig.*, Jun. 2012, pp. 1–3.

[46] T. Le, K. Mayaram, and T. Fiez, "Efficient Far-Field Radio Frequency Energy Harvesting for Passively Powered Sensor Networks," *IEEE J. Solid-State Circuits*, vol. 43, pp. 1287–1302, May 2008.

[47] E. Boshkovska, "Practical Non-Linear Energy Harvesting Model and Resource Allocation in SWIPT Systems," Master's thesis, University of Erlangen-Nuremberg, 2015. [Online]. Available: http://arxiv.org/abs/1602.00833

[48] S. Boyd and L. Vandenberghe, *Convex Optimization.* Cambridge University Press, 2004.

[49] M. Grant and S. Boyd, "CVX: Matlab Software for Disciplined Convex Programming, version 2.0 Beta," [Online] https://cvxr.com/cvx, Sep. 2013.

[50] H. Ju and R. Zhang, "Throughput Maximization in Wireless Powered Communication Networks," *IEEE Trans. Wireless Commun.*, vol. 13, pp. 418–428, Jan. 2014.

[51] E. Boshkovska, D. W. K. Ng, N. Zlatanov, and R. Schober, "Robust Resource Allocation for Wireless Powered Communication Networks with Non-linear Energy Harvesting Model," *submitted for possible publication*, 2016.

[52] E. Boshkovska, A. Koelpin, D. W. K. Ng, N. Zlatanov, and R. Schober, "Robust Beamforming for SWIPT Systems with Non-linear Energy Harvesting Model," in *Proc. IEEE Intern. Workshop on Signal Process. Advances in Wireless Commun.*, Jul. 2016.

[53] Y. Sun, D. W. K. Ng, J. Zhu, and R. Schober, "Multi-Objective Optimization for Robust Power Efficient and Secure Full-Duplex Wireless Communication Systems," *to appear in IEEE Trans. Wireless Commun.*, 2016.